Supplemental document for: **How Chemical Patterns Affect Equilibrium Droplet Shapes?**

Yanchen Wu, Fei Wang, Shaoping Ma, Michael Selzer, Britta Nestler

In this supplemental document, we present some details for the investigation of equilibrium droplet shapes on striped and chessboard-patterned surfaces under the influence of three factors: (a) droplet sizes, (b) contact angles, and (c) the ratios of the hydrophilic area to the hydrophobic one. In sections S. I-S. III, we illustrate the results of the energy landscape methods and the PF simulations for droplets on these two patterned surfaces. In section S. IV, we show the code for the energy landscape model.

S. I Droplet size

In this part, the contact angles on the hydrophilic and hydrophobic areas of the striped and chessboard-patterned surfaces are set as $60°$ and $120°$, respectively, i.e. $\theta_1 = 60°$, $\theta_2 = 120°$. The characteristic length in Eq. (7) is a constant value $L = 40$. With varying the droplet size R/L, we obtain the corresponding energy maps and simulation results.

Figure S1 presents the results from the analytical model and the PF simulation for droplets with different sizes on the striped patterned surface. From (I) to (III), the ratio R/L varies from 1 to 4.5. In each panel, (A) and (B) depict the surface energy landscapes in terms of a and b for droplets with base centers on position 1 and 2, respectively. The energy minima in the deep blue regions are indicated by different numbers and correspond to the snapshots of the PF simulation results labeled with the same number in (C). The blue and red stripes in the snapshots depict the hydrophilic and hydrophobic areas with width $L_{wet} = L_{dry} = L/2 = 20$. The red dashed ellipses with semi-axes a, b in (I)(C) represent the analytical results, which are obtained from the coordinates of the energy minima in the energy landscapes. It is observed that the analytical predictions of the energy landscapes have a good agreement with the simulation results. Moreover, as the ratio R/L increases from 1 to 4.5, the number of equilibrated droplets rises from 3 to 5.

Next, we turn to scrutinize the equilibrium shapes of droplets on a more complex pattern, the chessboard pattern. The surface energy landscapes and the corresponding snapshots of the equilibrated droplets from the PF simulations are illustrated in Figure S2 and Figure S3, respectively. In this scenario, we vary the droplet size from $R/L = 0.75$ to $R/L = 0.25$. The hydrophobic/hydrophilic square lattices (red/blue) have a width of $L_{dry} = L_{wet} = L/2 = 20$. Because of the high symmetry of the chessboard pattern, the elliptical base line of droplets may have a symmetric-axis which is rotated counterclockwise by $45°$ with respect to the horizontal direction, as sketched by the dot dashed line in Figure 2(c). The corresponding surface energy landscapes are calculated in a rotated system with $\delta_1' = (\delta_1 + \delta_2)/\sqrt{2}$ and $\delta_2' = (\delta_1 - \delta_2)/\sqrt{2}$ and the results are shown in Figure

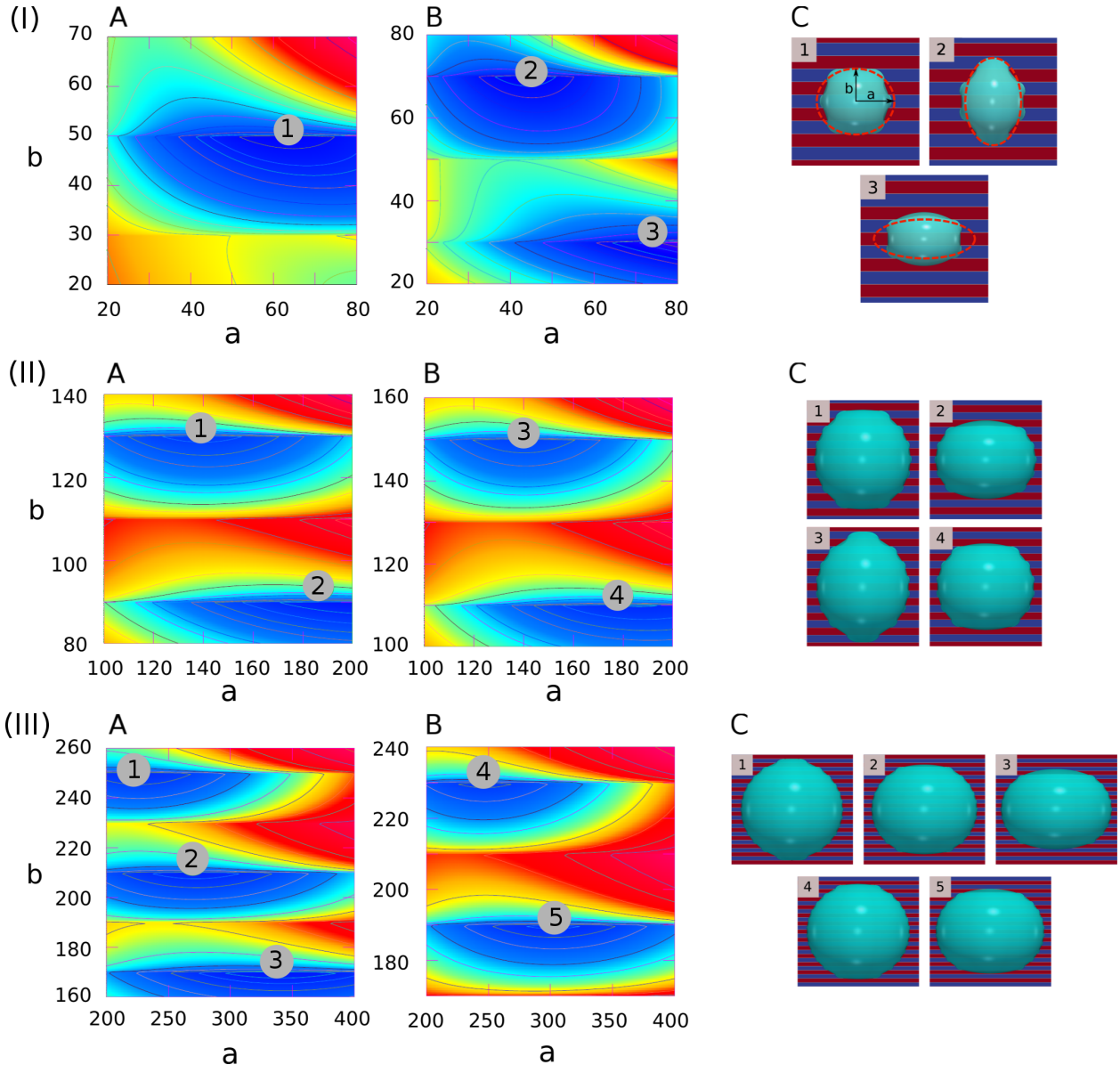

Figure S1: Surface energy landscapes for droplets with different sizes on the chemically striped patterned surfaces and the snapshots of the equilibrated droplets via PF simulations. (I) $R/L = 1$, (II) $R/L = 2.5$, (III) $R/L = 4.5$, The chemical heterogeneities are described by $f_1(r_b, \varphi)$ in Eq. (7) with the following parameters: $\gamma_m = 0$, $\gamma_0 = 0.5$, $\xi = 100$, $L = 40$, $\lambda = 0$. At equilibrium, the droplet base center stays either on $P_1(i = 1)$ (the center of the hydrophilic stripes, in blue color) or $P_2(i = 0)$ (the center of the hydrophobic stripes, in red color). The energy landscapes are accordingly calculated by using different values of i. The contour lines indicate the energy levels (red for high values and blue for low values). The energy minima are highlighted by different numbers in (A) and (B) in each panel, corresponding to the snapshots labeled with the same number in (C). The red dashed ellipses with semi-axes a, b in (I)(C) show the analytical results from the energy landscape method. Reproduced with permission from Ref.[1] Copyright 2019 American Physical Society.

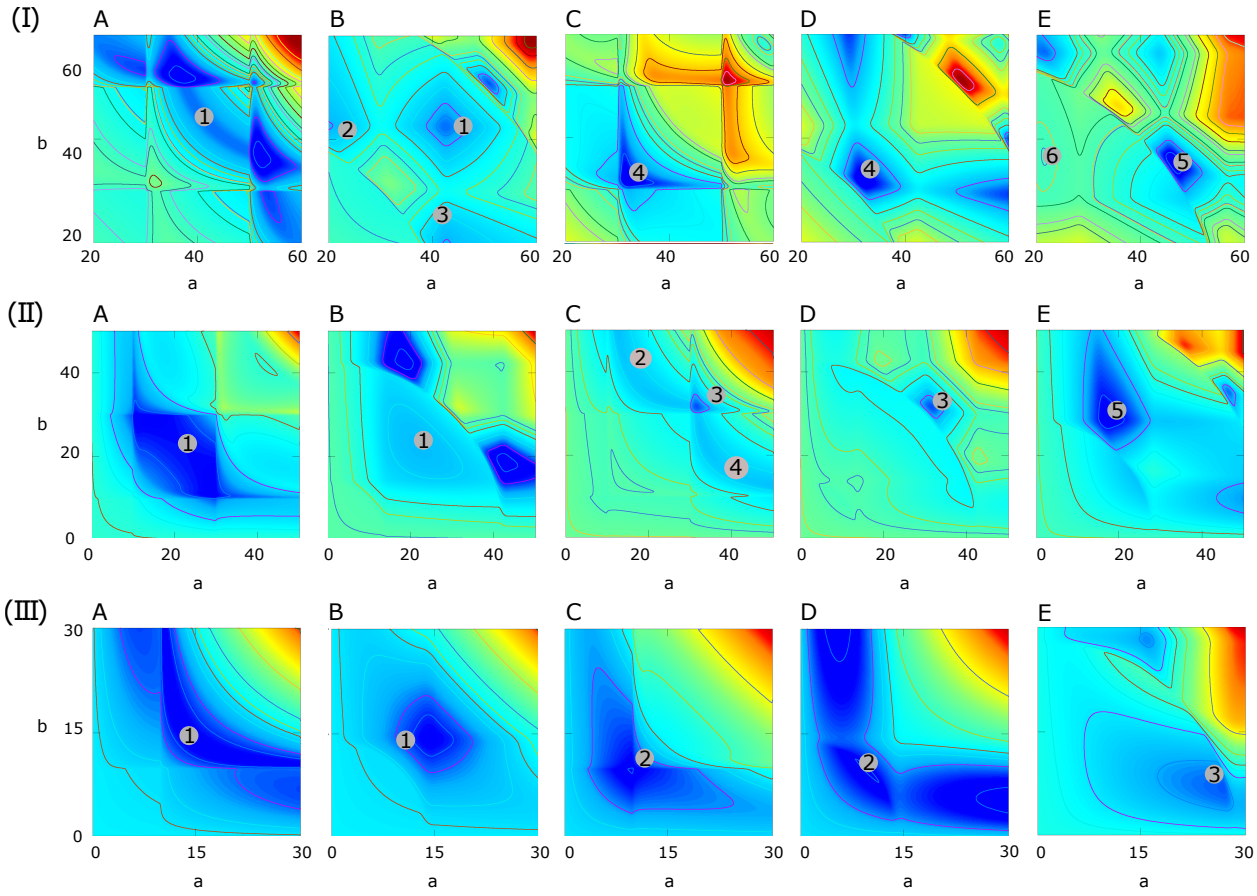

Figure S2: Surface energy landscapes for droplets with different sizes on the chessboard-patterned surfaces and the snapshots of the equilibrated droplets through PF simulations (I) $R/L = 0.75$, (II) $R/L = 0.5$, (III) $R/L = 0.25$. The chemical heterogeneities are described by $f_3(r_b, \varphi)$ in Eq. (7) with $\gamma_m = 0$, $\gamma_0 = 0.5$, $\xi = 100$, $L = 40$, $\lambda = 0$. The energy minima are illustrated by different numbers inside the gray circles. The equilibrated states at these energy minima are sequentially shown in Figure S3(I)-(III). The surface energy landscapes for (A)&(B), (C)&(D), and (E) correspond to droplets with base center positions on P_1, P_2, and P_3, respectively. In each panel, (A) and (C) describe the situation where a and b are in the horizontal and vertical directions, respectively. While (B), (D), and (E) depict a system which is rotated counterclockwise by $45°$. In the rotated system, δ_1 and δ_2 in $f_3(r_b, \varphi)$ are substituted by $\delta_1^{'}$ and $\delta_2^{'}$, respectively, with $\delta_1^{'} = (\delta_1 + \delta_2)/\sqrt{2}$ and $\delta_2^{'} = (\delta_1 - \delta_2)/\sqrt{2}$.

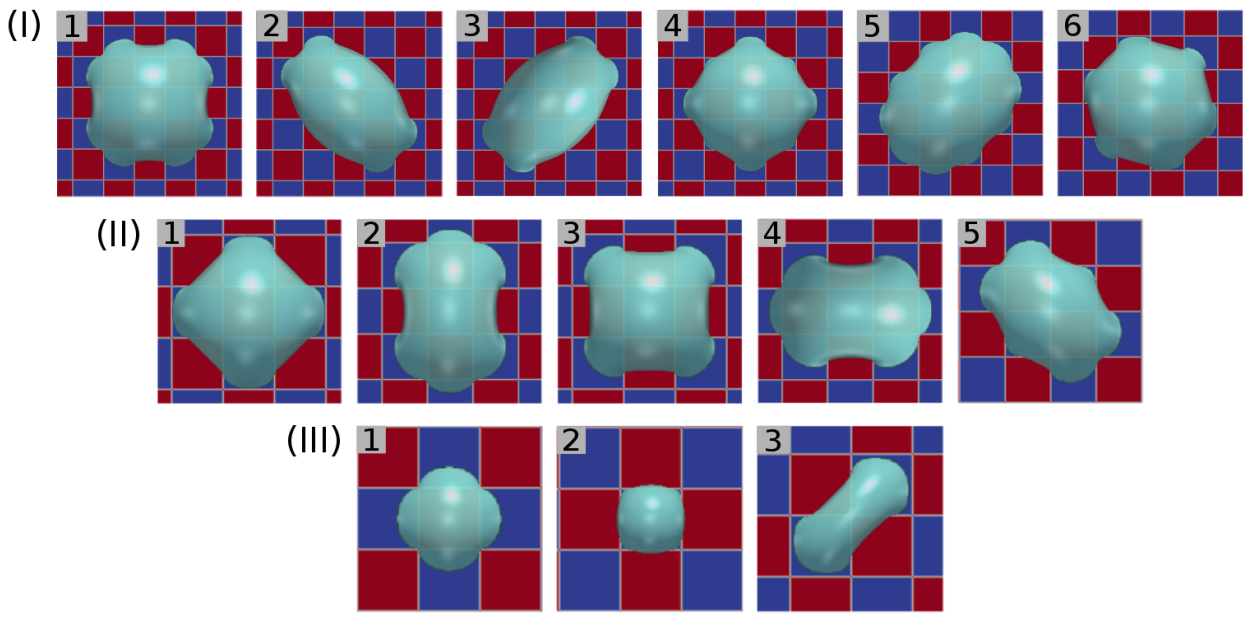

Figure S3: Snapshots for the equilibrated droplets with different sizes on the chessboard patterned surface via PF simulations (blue: hydrophilic, red: hydrophobic) (I) $R/L = 0.75$, (II) $R/L = 0.5$, (III) $R/L = 0.25$.

S2(B), (D), and (E) in each panel. Typical equilibrated droplet morphologies for the energy minima in Figure S2(I) (B) are displayed in Figure S3(I) (2) and (3). It is noteworthy that in Figure S2 (I) (C) and (D), which correspond to the non-rotated and rotated systems, respectively, the values of a and b are the same at the minimal energy states. These two energy minima actually predict an identical equilibrated shape, as shown in Figure S3(I) (4). The similar findings are observed in Figure S3(II) (1) and (3) as well as in Figure S3(III) (1) and (2). Similar to the striped and chocolate patterned surfaces, the increase in the droplet size leads to more equilibrium shapes.

S. II Contact angle

In this section, we investigate the equilibrated droplet shapes affected by the contact angles on the hydrophilic (θ_1) and hydrophobic (θ_2) areas. The chosen parameters for θ_1 and θ_2 are shown in Table 1. The characteristic length is constant $L = 40$. Droplets with the same size ($R/L = 1$) on the two chemically patterned surfaces are considered.

As three typical examples, Figure S4(I), (II), and (III) display the surface energy landscapes and the snapshots of the simulated equilibrium droplets on the striped-patterned surface for contact angle pairs $(30^\circ, 90^\circ)$, $(90^\circ, 150^\circ)$, $(120^\circ, 180^\circ)$, respectively. From (I) to (III) as $\overline{\theta}$ increases, the equilibrated morphologies tend to approach a spherical shape. Moreover, the number of the equilibrium states in (II) and (III) is less than that in (I).

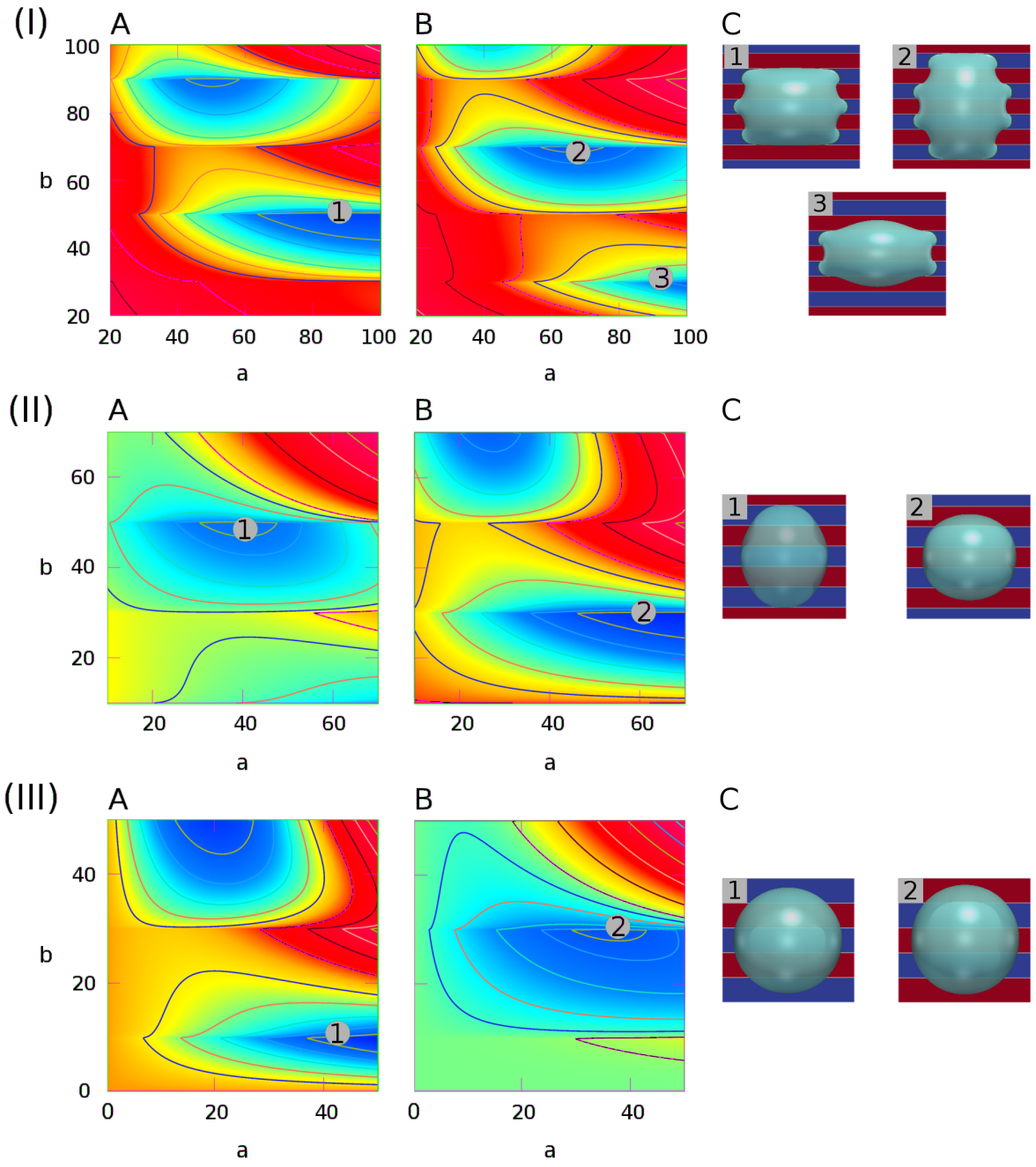

Figure S4: Surface energy landscapes for droplets on the striped patterned surfaces with different contact angles and the corresponding snapshots of the equilibrated droplets from the PF simulations. (I) $\theta_1 = 30°, \theta_2 = 90°$, (II) $\theta_1 = 90°, \theta_2 = 150°$, (III) $\theta_1 = 120°, \theta_2 = 180°$. The chemical heterogeneities are described by $f_1(r_b, \varphi)$ in Eq. (7) with $\xi = 100$, $L = 40$, $\lambda = 0$. The parameters γ_m, γ_0 are adjusted according to the contact angle pairs. The energy minima are indicated by different numbers, corresponding to the snapshots in (C) labeled with the same number. The surface energy landscapes for (A) and (B) delineate the situation where the droplet base center positions are on P_1 and P_2, respectively. (C) Snapshots of the equilibrated droplets through PF simulations (blue: hydrophilic, red: hydrophobic).

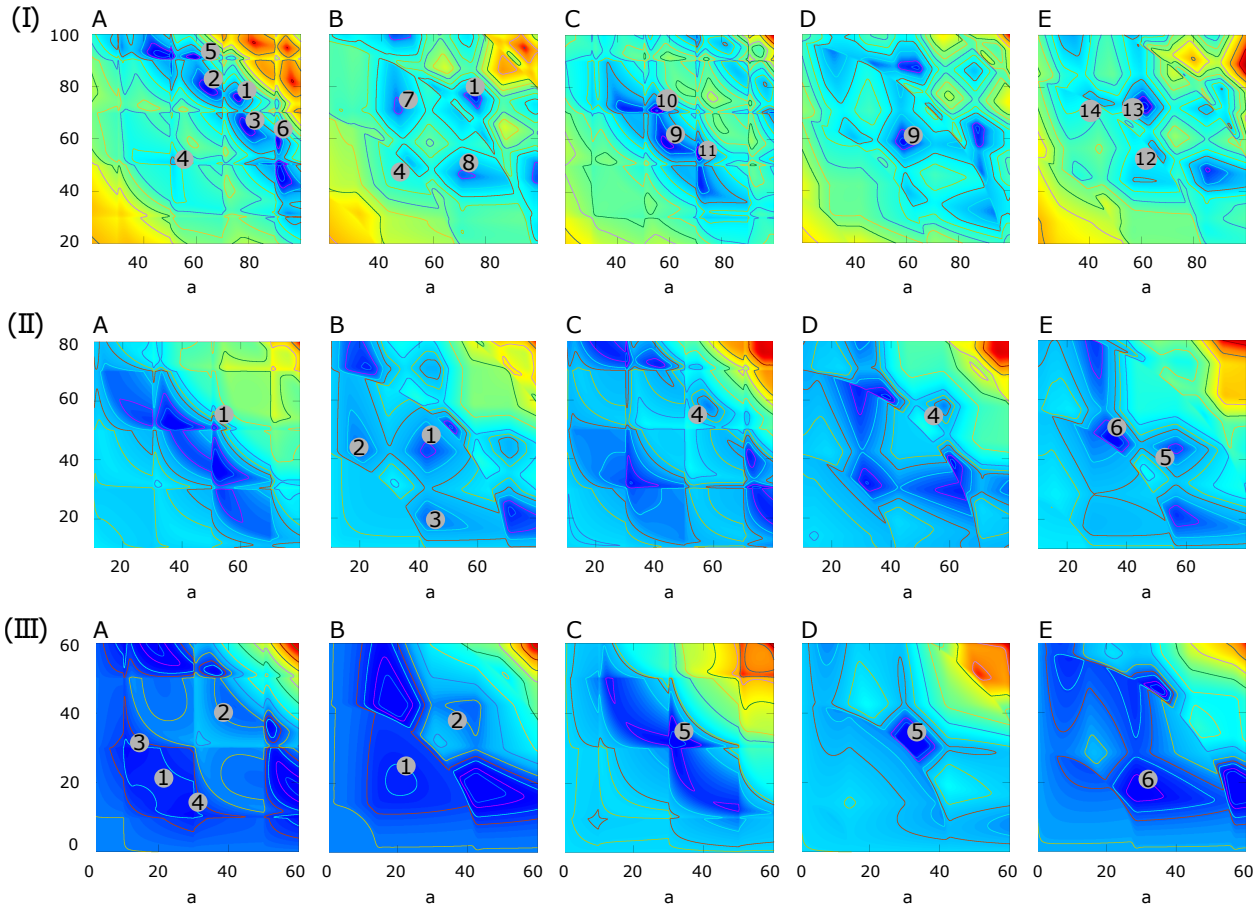

Figure S5: Surface energy landscapes for droplet on the chessboard-patterned surfaces with different contact angles and the corresponding snapshots of the equilibrated droplets through PF simulations (I) $\theta_1 = 30°, \theta_2 = 90°$, (II) $\theta_1 = 90°, \theta_2 = 150°$, (III) $\theta_1 = 120°, \theta_2 = 180°$. The chemical heterogeneities are described by $f_3(r_b, \varphi)$ in Eq. (7) with $\xi = 100$, $L = 40$, $\lambda = 0$. The parameters γ_m, γ_0 are modified according to the contact angle pairs. The energy minima are indicated by different numbers, corresponding to the snapshots in Figure S6(I)-(III) labeled with the same number. The surface energy landscapes for (A)&(B), (C)&(D), and (E) correspond to the droplet base center positions on P_1, P_2, and P_3, respectively. (A) and (C) describe the situation where a and b are in the horizontal and vertical directions, respectively While (B), (D), and (E) depict a system which is rotated counterclockwise by $45°$. In the rotated system, δ_1 and δ_2 in $f_3(r_b, \varphi)$ are substituted by δ_1' and δ_2', respectively, with $\delta_1' = (\delta_1 + \delta_2)/\sqrt{2}$ and $\delta_2' = (\delta_1 - \delta_2)/\sqrt{2}$.

We further turn to the chessboard pattern. Figure S5(I), (II), and (III) picture the surface energy landscapes for droplets on the chessboard patterned surfaces for contact angles $(30°, 90°)$, $(90°, 150°)$, and $(120°, 180°)$, respectively. In each panel, (A)&(B), (C)&(D), and (E) are for droplets with base centers on P_1, P_2, and P_3, respectively, among which (B), (D), and (E) are calculated in the rotated system. Figure S6 (I), (II), and (III) shows the snapshots of the simulated equilibrium droplet shapes, corresponding to the sequentially indicated energy minima in

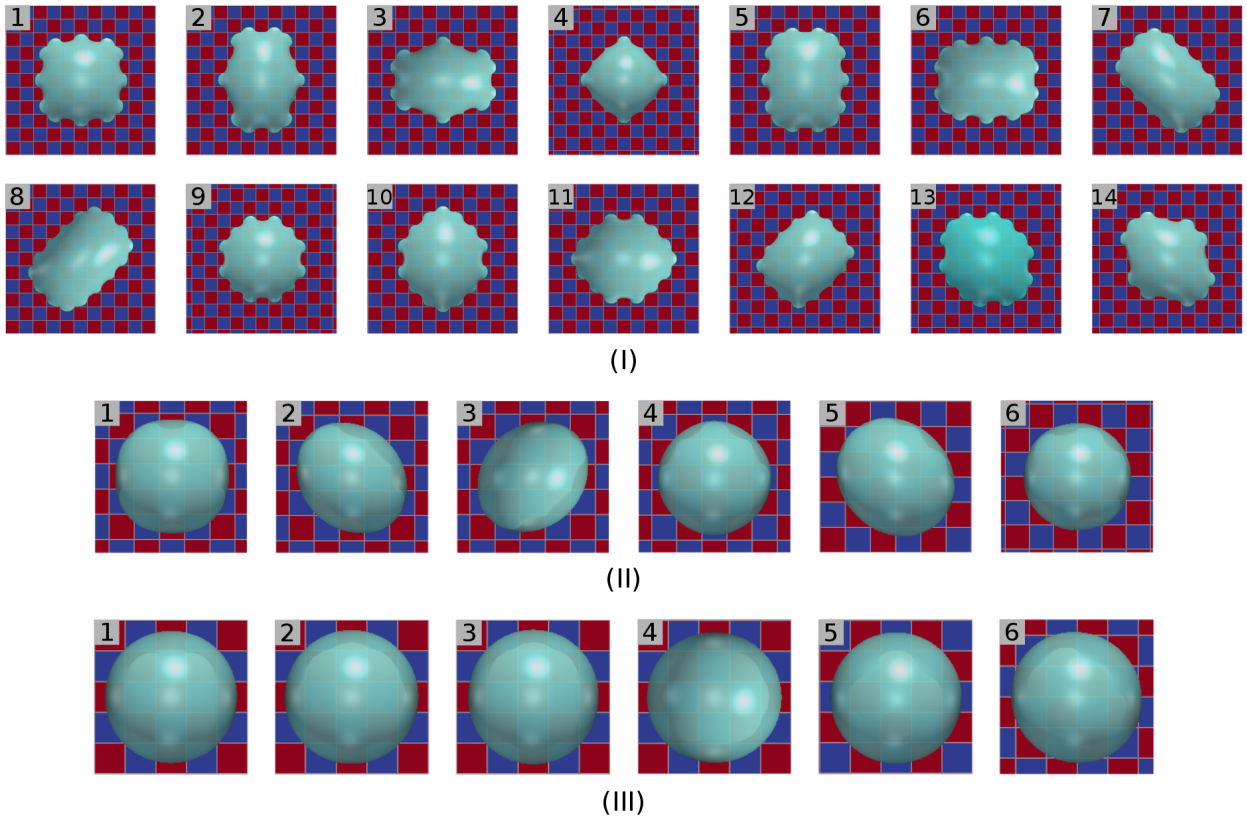

Figure S6: Snapshots of the equilibrated droplets on the chessboard patterned surfaces through PF simulations (blue: hydrophilic, red: hydrophobic) (I) $\theta_1 = 30°, \theta_2 = 90°$, (II) $\theta_1 = 90°, \theta_2 = 150°$, (III) $\theta_1 = 120°, \theta_2 = 180°$.

Figure S5 (I), (II), and (III), respectively. Since the density of the hydrophilic/hydrophobic lines for the chessboard patterned surfaces is higher than that of the striped and chocolate patterned surfaces, the energy landscapes become much more complex, which causes a substantial increase in the number of the equilibrated droplet shapes. The tendency that the evolution of the droplet morphologies towards a spherical shape with an increase in the average contact angle is also observed in this case.

S. III The ratio of the hydrophilic area to the hydrophobic area

The average contact angle $\overline{\theta}$ can also be adjusted by tuning the area ratio of the hydrophilic area to the hydrophobic area while fixing the intrinsic contact angles on these two areas. Here, we set the contact angles on the hydrophilic and hydrophobic areas as $\theta_1 = 60°$ and $\theta_2 = 120°$, respectively.

The area ratio of the hydrophilic area to the hydrophobic area is characterized by the parameter ν. For the striped surfaces with $\nu = 1:1,\ 1:2,\ 1:3$, the surface energy landscapes

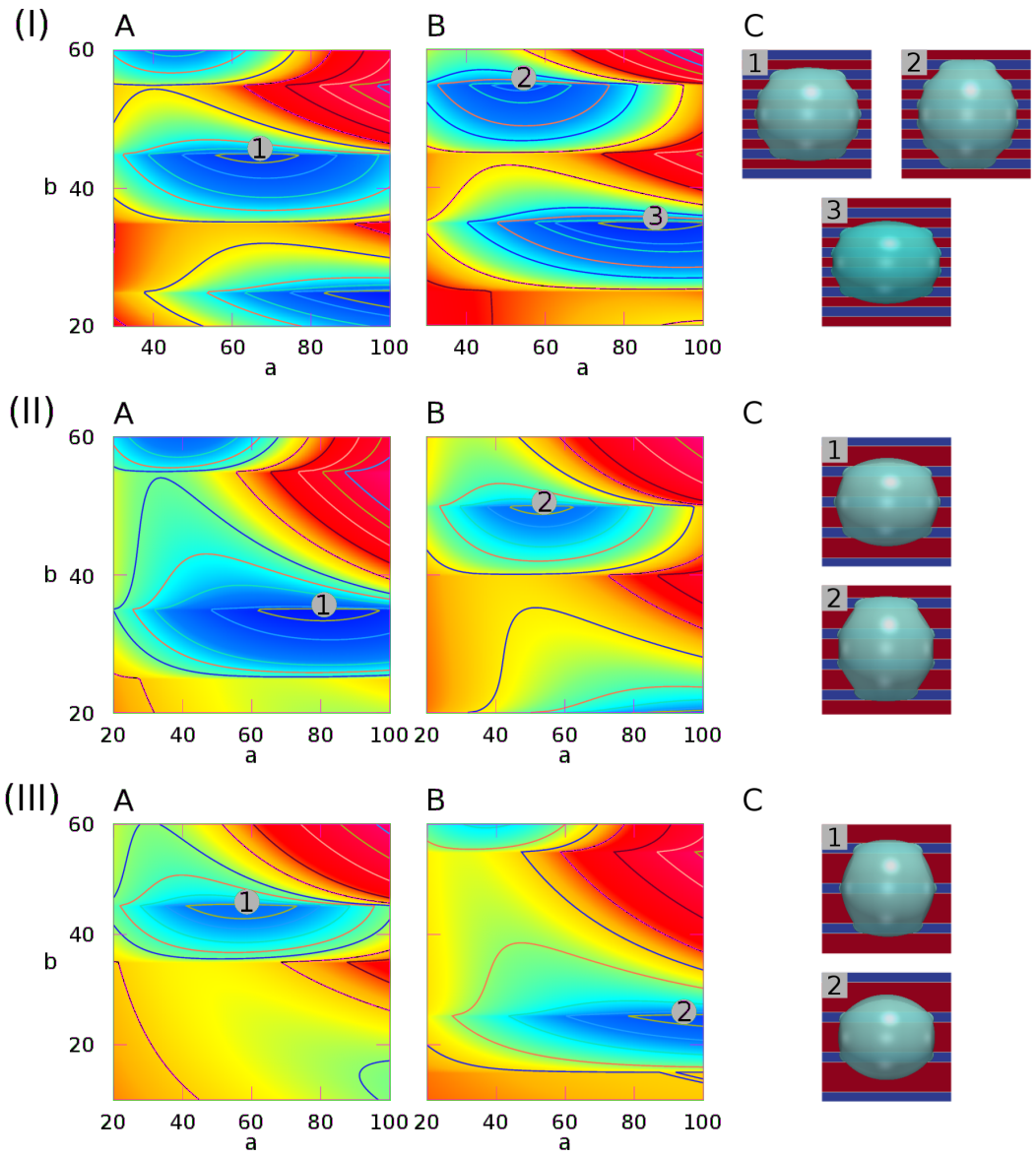

Figure S7: Surface energy landscapes for droplets on the striped surfaces with different area fractions of the hydrophilic and hydrophobic areas and the corresponding snapshots of equilibrated droplets through PF simulations. The ratios for (I) $\nu = 1:1$, (II) $\nu = 1:2$, (III) $\nu = 1:3$ correspond to three different setups with $(L = 20,\ \lambda = 0)$, $(L = 30,\ \lambda = \cos 60^\circ)$, $(L = 40,\ \lambda = \cos 45^\circ)$, respectively. The droplet size is set as $R = 40$. The chemical heterogeneities are described by $f_1(r_b, \varphi)$ in Eq (7) with $\gamma_m = 0$, $\gamma_0 = 05$, $\xi = 100$. The energy minima are marked by different numbers, corresponding to the snapshots in (C) labeled with the same number. The energy landscapes in (A) and (B) are for the situations where the droplet base center positions are on P_1 and P_2, respectively. (C) Snapshots of the equilibrated droplets via simulations (blue: hydrophilic, red: hydrophobic).

and the snapshots of the equilibrated droplets from the PF simulations are shown in Figure S7 (I), (II), and (III), respectively. A good agreement between the energy landscape model and the PF model is observed. As ν decreases, the equilibrated droplet becomes spherical successively and N decreases.

S. IV Code for the energy landscape model

In this section we present the code for calculating the surface energy landscapes. For different patterned surfaces, the corresponding descriptions of f_k are used.

Listing 1: surfaceEnergy.m

```
function y=f(phi)
global prop;
%(gamma_m,gamma_0) -> (theta_1,theta_2), here (pi/3,2*pi/3)
gamma_m = 0;
gamma_0 = 0.5;
 L      = 40; %L is the characteristic length


r   = (prop.a_f*prop.b_f)/sqrt(prop.a_f**2*sin(phi)**2
+prop.b_f**2*cos(phi)**2); %r is here base radius. See Eq.(3)

%gab_difference is f_k=gamma_ls - gamma_gs (k=1,2,3) see Eq.(7)

%striped-pattern, here xi=100
gab_difference = gamma_m+gamma_0*tanh(100*
cos(2*pi*r*cos(phi)/L));

%chcolate-pattern
%gab_difference = gamma_m + gamma_0*tanh(100*(cos(2*pi*r*cos(phi)
   /L)
%*cos(2*pi*r*sin(phi)/L)
%-cos(2*pi*r*cos(phi)/L)
%-cos(2*pi*r*sin(phi)/L)));

%chessboard-pattern no rotation
%gab_difference = gamma_m+gamma_0*tanh(100*
%cos(2*pi*r*cos(phi)/L)*
%cos(2*pi*r*sin(phi)/L));

%chessboard-pattern rotation 45 deg
%r*cos(phi)-->sqrt(0.5)*r*(sin(phi)+cos(phi))
```

```
%r*sin(phi)-->sqrt(0.5)*r*(sin(phi)-cos(phi))
%gab_difference = gamma_m + gamma_0*tanh(100*
%cos(2*pi*sqrt(0.5)*r*(sin(phi)+cos(phi))/L)
%*cos(2*pi*sqrt(0.5)*r*(sin(phi)-cos(phi))/L));

%y is to calculate surface energy in liquid-solid contact area
%part (bottom). See Eq.(8)
y = 0.5*r**2*gab_difference;

endfunction

function z=cap(fai)
global prop;

r_numerator   = (prop.a_f*prop.b_f);
r_denominator = sqrt(prop.a_f**2*sin(fai)**2+prop.b_f**2*cos(fai)
   **2)
r             = r_numerator /r_denominator; %r is base radius
r_c           = (r**2+prop.h_f**2)/(2*prop.h_f); %r_c is
   curvature radius. See Eq.(2)
beta          = acos((r_c-prop.h_f)/r_c); %beta see Eq.(6)
z             = r_c**2*(1-cos(beta)); %z is to calculate surface
   energy in liquid-gas interface
%part (cap).

endfunction

R = 40;
V = (4/3)*pi*R**3;
L = 40;

global prop;
fp=fopen("sigma_r40.dat",'w');

for a=0.5:1:120
  for b=0.5:1:120
    prop.a_f            = a;
    prop.b_f.           = b;
    h                   = fsolve(@(x) (pi/6)*x*(3*a*b+x**2)-V,1);
    prop.h_f            = h;
    surface_bottom      = 4*quad("f", 0, pi/2); %surface energy
       in A_ls
```

```
69      surface_ellipse_cap = 4*quad("cap", 0, pi/2);  %surface
           energy in  A_lg
70      sigma               = surface_bottom + surface_ellipse_cap; %
           total surface energy
71      fprintf(fp,'%f %f %f\n', a, b, sigma);
72    endfor
73    fprintf(fp,'\n');
74  endfor
75
76  fclose(fp);
```

References

1. Y. Wu, F. Wang, M. Selzer and B. Nestler, *Phys. Rev. E*, 2019, **100**, 041102.